

NASA Technical Memorandum 102331

# Speckle Interferometry Using Fiber Optic Phase Stepping

Carolyn A. Mercer and Glenn Beheim  
*Lewis Research Center*  
*Cleveland, Ohio*

Prepared for the  
Symposium on Optical and Optoelectronic Applied Science and Engineering  
sponsored by the Society of Photo-Optical Instrumentation Engineers  
San Diego, California, August 6-11, 1989



(NASA-TM-102331) SPECKLE INTERFEROMETRY  
USING FIBER OPTIC PHASE STEPPING (NASA.  
Lewis Research Center) 9 p CSCL 14B

N89-27999

Unclas  
G3/35 0224992

# Speckle interferometry using fiber optic phase stepping

Carolyn R. Mercer and Glenn Beheim

National Aeronautics and Space Administration  
Lewis Research Center  
21000 Brookpark Road, Cleveland, Ohio 44135

## ABSTRACT

A system employing closed-loop phase-stepping is used to measure the out-of-plane deformation of a diffusely reflecting object. Optical fibers are used to provide reference and object beam illumination for a standard two-beam speckle interferometer, providing set-up flexibility and ease of alignment. Piezoelectric fiber-stretchers and a phase-measurement/servo system are used to provide highly accurate phase steps. Intensity data is captured with a charge-injection-device camera, and is converted into a phase map using a desktop computer.

The closed-loop phase-stepping system provides  $90^\circ$  phase steps which are accurate to  $0.02^\circ$ , greatly improving this system relative to open-loop interferometers. The system is demonstrated on a speckle interferometer, measuring the rigid-body translation of a diffusely reflecting object with an accuracy of  $\pm 10^\circ$ , or roughly  $\pm 15$  nm. This accuracy is achieved without the use of a pneumatically mounted optics table.

## 1. INTRODUCTION

Speckle interferometry is a technique which measures deformations of diffusely reflecting objects using low spatial resolution detectors.<sup>1</sup> It is difficult to accurately interpolate between the resultant interferometric fringes, so phase-stepping techniques have been applied to speckle interferometry to provide direct digital processing of the phase measurements.<sup>2</sup> The accuracy of these measurements can be limited by phase stepping errors.<sup>3</sup> The phase modulator, usually a mirror mounted on a piezoelectric transducer, must first be calibrated, a procedure frequently complicated by transducer nonlinearity and hysteresis, as well as sensitivity drift caused by temperature fluctuations and changes in the optical layout. Nonuniform mirror motion, which causes the magnitude of the phase steps to vary as a function of position, is another common error source. Open-loop phase stepping systems are also subject to errors caused by random phase variations produced by vibration, temperature fluctuations, and air currents.

This paper describes a phase-stepping speckle interferometer based on a highly accurate closed-loop phase-stepping system which uses a synchronous phase detection technique<sup>4</sup> and an all-fiber optical system<sup>5</sup> as described in Ref. 6. This phase control technique compensates for both phase modulator errors and random phase shifts caused by environmental disturbances of the optical fibers. The single-mode optical fibers provide spatially uniform phase fronts and a flexible optical delivery system. The phase-stepping speckle interferometer is used to measure the out-of-plane deflection of an aluminum blade. The measurements indicate the direction as well as the magnitude of displacement, and are made without using a pneumatically mounted vibration isolation table, demonstrating the stability that can be achieved with this system.

The experimental apparatus is described first, followed by the method of data acquisition. Finally, phase measurements showing the displacement of an object are presented as phase maps, histograms and plots.

## 2. EXPERIMENTAL APPARATUS

A schematic of the optical system is shown in Fig. 1. The entire system is mounted on a honeycomb optical table without pneumatic vibration dampening. The dashed line represents an enclosure built around the speckle interferometer to reduce the effects of air turbulence.

The object under study (OBJ) is a metal blade covered with retroreflective tape to increase its reflectivity. The object is mounted on a piezoelectrically-driven translation stage (PZT3) to provide object displacement along the axis shown by the double-headed arrow. Light from a fiber ( $F_{obj}$ ) illuminates the object, which is imaged with unity magnification through a 120 mm lens (L2) onto a 120 by 120 pixel charge-injection-device camera (CID). An aperture (A) is stopped down to approximately  $f/60$ , creating image-plane speckles larger than the camera's 28  $\mu\text{m}$  detector elements. To maximize the reflected light that passes through the aperture, the object is placed so that its normal bisects  $\alpha$ , the  $40^\circ$  angle that the object beam makes with the camera's optical axis.

Light emitted from another fiber ( $F_{ref}$ ) serves as a reference wavefront and is diverted to the camera by a 50:50 beamsplitting cube (BS). A lens/pinhole combination (L3/PH) creates a spatially filtered spherical wave which, to the camera, appears to originate from aperture A. The distances between each output fiber face and the camera are equal to within the 2 cm coherence length of the argon ion laser.

The fiber optic system shown in Fig. 1 serves as a light delivery system for the speckle-interferometer and also provides for highly accurate phase stepping. Light from an argon ion laser operating at 514.5 nm is coupled through a lens (L1) into one leg ( $F_{in}$ ) of a variable-ratio fiber-optic coupler (FC). This light is split into the path length matched 10 m long output fibers  $F_{obj}$  and  $F_{ref}$  used in the speckle interferometer. These fibers are single-mode nonpolarization-preserving fibers. Each output fiber is wrapped tightly around a piezoelectric transducer (PZT1 and PZT2) forming a fiber optic phase-controller on each arm of the interferometer. A portion of the light traveling through each output fiber is reflected at the fiber's end face, and travels back through the coupler. The reflected light from each fiber combines interferometrically within the fourth leg of the fiber-optic coupler ( $F_{sig}$ ) and is detected by a photodiode (PD). Defining the one-way phase delay of the light traveling through fibers  $F_{obj}$  and  $F_{ref}$  to be  $\theta_{obj}$  and  $\theta_{ref}$  respectively, the current generated by PD can be described as:

$$i_{pd} = K_{pd} I_0 [1 + m \cos(2\theta_{ref} - 2\theta_{obj})] \quad (1)$$

where  $K_{pd}$  is the sensitivity of the photodetector,  $I_0$  is the mean detected intensity, and  $m$  is the fringe visibility. A 10 kHz sinusoidal voltage applied to PZT1 modulates  $i_{pd}$  for synchronous detection by the closed-loop phase-control system; the modulated current is described by:

$$i_{pd} = K_{pd} I_0 \{1 + m \cos[2\theta - 2\beta \sin(\omega t)]\} \quad (2)$$

where  $\theta = (\theta_{ref} - \theta_{obj})$ , and  $\beta$  and  $\omega$  are the amplitude and frequency of the phase modulation, respectively.

A block diagram of the phase-control system is shown in Fig. 2. An oscillator (OSC) generates the modulation signal which drives PZT1. A lock-in amplifier (LOCK-IN)

compares the amplified signal from PD to the oscillator's driving frequency and generates a voltage ( $E_1$ ) which is described by:<sup>6</sup>

$$E_1 = C \sin(2\theta) \quad (3)$$

where  $C = K_{LI} K_{AMP} K_{PD} I_0 m J_1(2\beta)$ ,  $K_{LI}$  is the gain of the lock-in amplifier,  $K_{AMP}$  is the sensitivity of the current-to-voltage converter preamp, and  $J_1()$  is the first order Bessel function. An integrator (INT) and a high-voltage amplifier (AMP) integrate and amplify  $E_1$  for use as an error signal. This error signal drives PZT2, changing the optical path length of  $F_{ref}$  until  $E_1$  is nulled. When  $E_1$  is nulled,  $\theta$  equals either  $0^\circ$  or  $180^\circ$ , depending on initial conditions. Changing the loop polarity allows  $\theta$  to be set to  $90^\circ$  or  $270^\circ$ .<sup>6</sup> This sign change is accomplished with a computer controlled switch (SW2). In order to select between the two allowable values of  $\theta$ , the initial conditions can be set by temporarily deactivating the feedback loop with a switch (SW1) and applying an offset voltage to PZT1 to coarsely step the phase to the desired value, and then reactivating the phase-control system within 20 msec to lock onto and maintain the correct phase setting. This computer-controlled offset voltage is applied with a digital-to-analog converter (D/A). In this way, the relative phase between the light at the output fiber faces can be set to any multiple of  $90^\circ$ , i.e.,  $\theta_n = (n - 1) (90^\circ)$  where  $n = 1, 2, 3$ , or  $4$ . The root mean square phase step error was determined to be  $0.02^\circ$  by measuring the standard deviation in  $E_1$  and using Eq. (3).<sup>6</sup>

### 3. DATA ACQUISITION

The out-of-plane displacement of the object was measured using the fiber optic phase-stepping interferometer. A voltage applied to PZT3 moved the object along the optical axis as shown by the double-headed arrow in Fig. 1. The phase of the light reflected off the surface of the object relative to the reference wave was measured before and after the object was translated, and a phase map  $\phi(x,y)$  was calculated showing the out-of-plane component of the distance that the object moved.

In order to measure the phase of the light reflected off of the object relative to the reference wave, four images were acquired by the CID camera with the relative phase  $\theta$  stepped by  $90^\circ$  between exposures. The intensity field detected by the CID camera can be described as:

$$I_n(x,y) = I_0(x,y)\{1 + m(x,y)\cos[\phi(x,y) + \theta_n]\} \quad (4)$$

where  $I_0(x,y)$  is the average intensity detected by pixel  $(x,y)$ ,  $m(x,y)$  is the corresponding visibility, and  $\phi(x,y)$  is the relative phase of the object and reference waves caused by optical path differences between the output fibers' end faces and the camera. Four intensity maps  $I_n(x,y)$  are recorded while the object was in a reference position, and then four more were recorded after the object had been moved. The intensity maps were stored on a desktop computer via an eight-bit A/D card.

Phase stepping and object translation were computer controlled, while an operator acquired images after each phase step. In order to provide adequate operator response time, there was a 5 sec pause between each phase step. A 10 sec delay was included to move the object and allow it to settle, for a total acquisition time of 60 sec. No attempt was made to minimize this time; 1/30 sec for each frame capture and perhaps a 1 sec pause for object translation could reduce this time to less than 3 sec.

The relative phase  $\varphi(x,y)$  is determined at each pixel by using the standard phase-stepping relation:<sup>7</sup>

$$\varphi(x,y) = \tan^{-1} \left\{ \frac{[I_4(x,y) - I_2(x,y)]}{[I_1(x,y) - I_3(x,y)]} \right\}. \quad (5)$$

The phase at a give point was calculated only if the signal modulation ( $2I_0m$ ) exceeded a threshold  $C_{th}$  where:<sup>8</sup>

$$2I_0m = \left\{ [I_1(x,y) - I_3(x,y)]^2 + [I_4(x,y) - I_2(x,y)]^2 \right\}^{1/2} \quad (6)$$

and the threshold constant  $C_{th}$  was chosen to minimize the deviation in the calculated phase  $\varphi$  while maximizing the number of valid pixels.

#### 4. RESULTS

At each validated point, the initial phase was subtracted from the final phase to determine the phase difference  $\Delta\varphi$  representing the motion of the object caused by voltage applied to PZT3. Figure 3 shows the phase difference measured across the 120 by 120 pixel array when 19.2 V was applied to PZT3. The threshold constant  $C_{th}$  was set to 1/20 of the saturation intensity. The shaded pixels show the structure of the recorded speckle pattern; the level of grey indicates the value of  $\Delta\varphi$ . Black areas represent invalid pixels. Slightly fewer than one-half of the pixels were considered invalid, primarily because more than one speckle was present at those pixels.

The phase shifts calculated at each pixel are shown in Fig. 4 as histograms for each of four voltages applied to PZT3. This data shows that the object moved away from the detector when a voltage was applied,  $360^\circ$  represents no motion and  $0^\circ$  indicates a displacement of  $\lambda/[2 \cos^2(\alpha/2)]$  away from the detector. The widths of these histograms show that the uncertainty in the measured phase across the surface of the blade is about  $10^\circ$  rms. The average phase steps across the detector array were computed from the histograms. These average phase steps were measured eight times at each of nine voltages applied to PZT3. This data plotted in Fig. 5 shows that the error in the repeated measurement of the displacements was  $6.8^\circ$  on the average, and was as large as  $14^\circ$ . The data was fit to a straight line and had a correlation coefficient of 0.988, showing that PZT3 was only approximately linear over the region that it was traversed. One data point lies far off of the general curve. This was the only point which passed the modulation threshold and yielded an incorrect measurement, in fact, the histogram for this point was very narrow. The most likely explanation for this erroneous point is operator error, probably caused by acquiring an image at the wrong time. Four of the 72 phase measurements were corrected for a  $180^\circ$  phase stepping error. This error can be caused by any disturbance which alters the phase  $\theta$  by more than  $180^\circ$  during the 20 msec that the phase control system is under open-loop control.

When nonrigid-body translation is to be measured, the phase at a single pixel can be tracked. Figure 6 shows the phase measured as a function of applied voltage for three randomly selected pixels. Although only three pixels are shown, all of the valid pixels show the same trend.

## 5. CONCLUSION

A fiber optic phase stepping interferometer was demonstrated by measuring the out-of-plane motion of a rigid body with  $\pm 10^\circ$  accuracy without using a pneumatically mounted optical table. This system's inherent advantages include the flexibility of a fiber optic based optical configuration and the accuracy of closed-loop phase control.

## 6. REFERENCES

1. R. Jones and C. Wykes, Holographic and Speckle Interferometry, Chapter 3, Cambridge University Press, Cambridge (1983).
2. D.W. Robinson and D.C. Williams, "Digital Phase Stepping Speckle Interferometry," *Optics Commun.* 57(1), 26-30 (1986).
3. C. Ai and J.C. Wyant, "Effect of Piezoelectric Transducer Nonlinearity on Phase Shift Interferometry," *Appl. Opt.* 26(6), 1112-1116 (1987).
4. D.B. Neumann and H.W. Rose, "Improvement of Recorded Holographic Fringes by Feedback Control," *Appl. Opt.* 6(6), 1097-1104 (1967).
5. M. Corke, J.D.C. Jones, A.D. Kersey and D.A. Jackson, "All Single-Mode Fibre Optic Holographic System with Active Fringe Stabilisation," *J. Phys. E.* 18(3), 185-186 (1985).
6. C.R. Mercer and G. Beheim, "Active Phase Compensation System for Fiber Optic Holography," NASA TM-101295 (1988).
7. J.C. Wyant, "Use of an ac Heterodyne Lateral Shear Interferometer with Real-Time Wavefront Correction Systems," *Appl. Opt.* 14(11), 2622-2626 (1975).
8. K. Creath, "Phase-Shifting Speckle Interferometry," International Conference on Speckle, SPIE Proc. 556, H.H.Arsenault, Ed., 337-346 SPIE, Bellingham, WA, (1985).

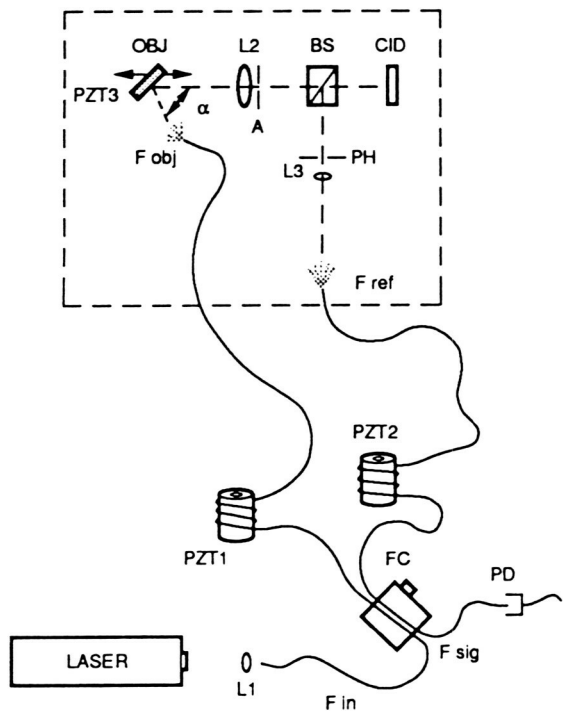


Figure 1. - Optical system for phase-stepping speckle interferometry.

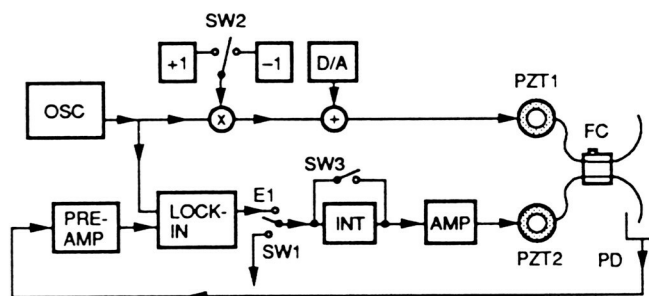


Figure 2. - Phase-control electronics.

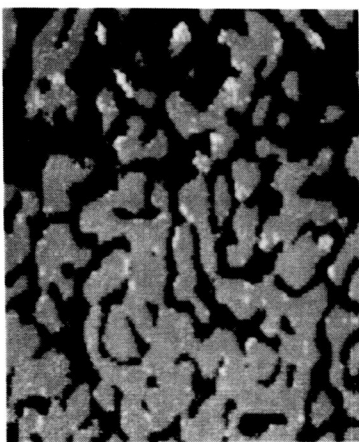


Figure 3. - 120 x 120 pixel phase map, 19.2 volts applied to PZT3.

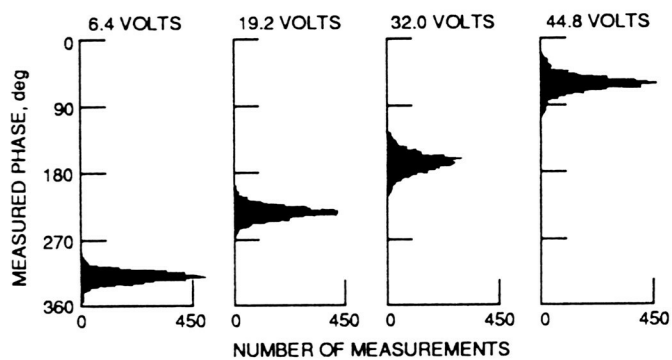


Figure 4. - Phase histograms for four applied voltages.

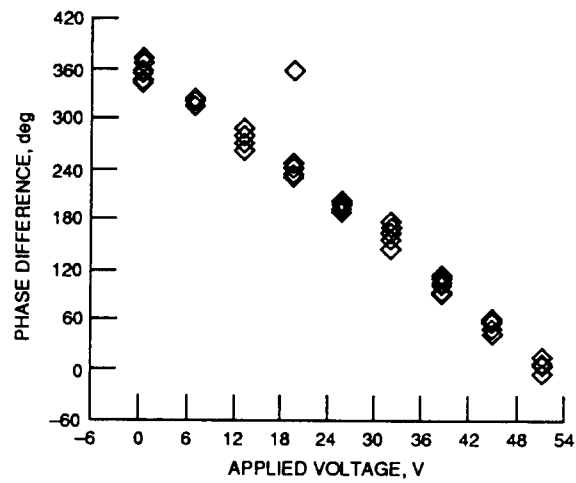


Figure 5. - Measured phase difference vs. voltage applied to PZT3.

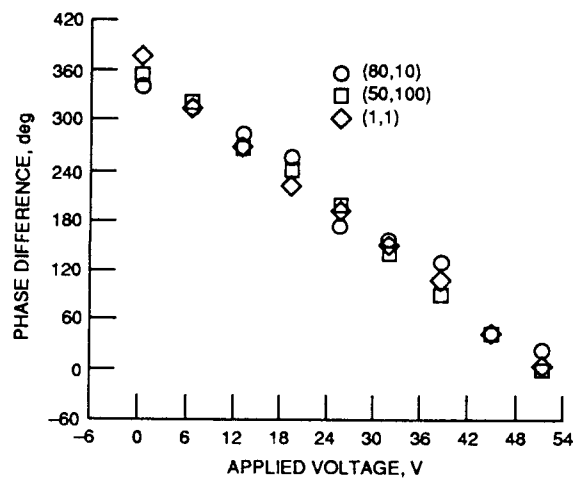


Figure 6. - Phase measurement at three pixels.



## Report Documentation Page

1. Report No. NASA TM-102331		2. Government Accession No.		3. Recipient's Catalog No.	
4. Title and Subtitle Speckle Interferometry Using Fiber Optic Phase Stepping				5. Report Date	
				6. Performing Organization Code	
7. Author(s) Carolyn R. Mercer and Glenn Beheim				8. Performing Organization Report No. E-5040	
				10. Work Unit No. 582-01-11	
9. Performing Organization Name and Address National Aeronautics and Space Administration Lewis Research Center Cleveland, Ohio 44135-3191				11. Contract or Grant No.	
				13. Type of Report and Period Covered Technical Memorandum	
12. Sponsoring Agency Name and Address National Aeronautics and Space Administration Washington, D.C. 20546-0001				14. Sponsoring Agency Code	
15. Supplementary Notes Prepared for the Symposium on Optical and Optoelectronic Applied Science and Engineering sponsored by the Society of Photo-Optical Instrumentation Engineers, San Diego, California, August 6-11, 1989.					
16. Abstract <p>A system employing closed-loop phase-stepping is used to measure the out-of-plane deformation of a diffusely reflecting object. Optical fibers are used to provide reference and object beam illumination for a standard two-beam speckle interferometer, providing set-up flexibility and ease of alignment. Piezoelectric fiber-stretchers and a phase-measurement/servo system are used to provide highly accurate phase steps. Intensity data is captured with a charge-injection-device camera, and is converted into a phase map using a desktop computer. The closed-loop phase-stepping system provides 90° phase steps which are accurate to 0.02°, greatly improving this system relative to open-loop interferometers. The system is demonstrated on a speckle interferometer, measuring the rigid-body translation of a diffusely reflecting object with an accuracy of <math>\pm 10^\circ</math>, or roughly 15 nanometers. This accuracy is achieved without the use of a pneumatically mounted optics table.</p>					
17. Key Words (Suggested by Author(s)) Speckle; Interferometry; Fiber optics; Phase stepping; Closed loop			18. Distribution Statement Unclassified—Unlimited Subject Category 35		
19. Security Classif. (of this report) Unclassified		20. Security Classif. (of this page) Unclassified		21. No of pages 8	
				22. Price* A02	